MT 25

25th International Conference on Magnet Technology

# High Gradient Nb3Sn Quadrupole Demonstrator MKQXF Engineering Design

**ID:MT25-Wed-Af-Po3.01-02**


Kokkinos Charilaos[1], Karppinen Mikko[2]

1. FEAC Engineering P.C., Afstralias Str. 61, 26442, Patras, Greece
2. CERN, CH-1211 Genève 23, Switzerland



## Abstract

The future upgrades of the CERN accelerator chain along with the future high energy colliders, notably the FCC, will require high gradient quadrupoles. As part of the HL-LHC project, the 11T Dipole was the first Nb3Sn magnet designed from the beginning to be compatible with the accelerator requirements and industrial production. It is based on the "pole-loading" concept, in which the Ti-alloy pole is not part of the coil, but inserted during the assembly process. This allows shimming at the pole and uses the collars more efficiently for creating the coil pre-stress. MKQXF is the further development of the "pole-loading" concept for Nb3Sn quadrupoles. The pole region of the coils is identical to the 11T dipole and the collared coil is based on dipole-type collars. This concept can easily be extended to any length and applied on both 1-in-1 and 2-in-1 configurations. For benchmarking purposes and to compare with the present baseline design of the HL-LHC IR quadrupole QXF, based on bladder-and-key concept, this conceptual study was made with identical coils and quasi-identical magnetic characteristics. The design features 140 T/m gradient in 150 mm coil aperture. This paper describes the design concept of MKQXF and the fully 2D & 3D parametric multi-physics finite element model (FEM), including the end regions. The design optimization is described and the optimized assembly parameters and the effect of the manufacturing tolerances are presented.


## Mechanical structure

This conceptual study was made with identical coils and quasi-identical magnetic characteristics (*Figure 1*) as the HL-LHC IR quadrupole QXF [3], based on the bladder-and-key concept.

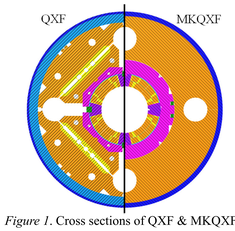


*Figure 1*. Cross sections of QXF & MKQXF

The removable pole in the pole-loading concept allows shimming at the pole and uses the collars more efficiently for creating the coil pre-stress (*Figure 2*).

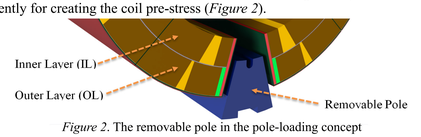


*Figure 2*. The removable pole in the pole-loading concept

The main features of the MKQXF design are illustrated in *Figure 3*.

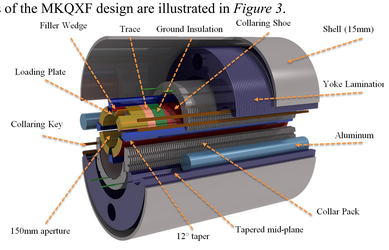


*Figure 3*. Exploded view of MKQXF

In the horizontal plane the pole wedge has a 12° taper such that the collars push the wedge radially in during the collaring (*Figure 4*). The stress relief notch in the pole wedges is essential for the stress distribution of the inner layer pole-turns.The laminated iron yoke is made of two halves with a horizontal split (*Figure 4*). The yoke midplane is tapered such that with the contact on the inner radius the outer radius has a 0.05 mm gap in the free state.

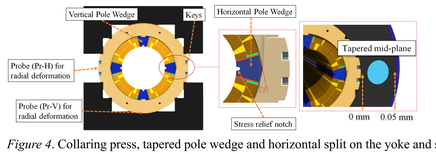


*Figure 4*. Collaring press, tapered pole wedge and horizontal split on the yoke and shell

## 2D Model

### Magnetic Analysis

The electromagnetic model is analyzed in MAXWELL, ROXIE [4] & PITHIA [5] to compare results between the Finite Element (FEM) and the Boundary Element Method (BEM). The magnetic field at 11.81 T is shown at *Figure 5* and the magnetic flux density at the nominal (140 T/m) and the ultimate (155 T/m) design gradient is shown in *Table 1*.

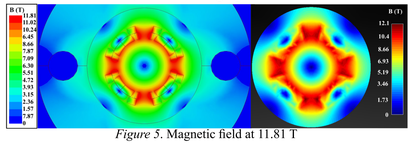


*Figure 5*. Magnetic field at 11.81 T

| Magnetic Field Gradient | $I_{ss}$ | $B_{max}$ | |
|---|---|---|---|
| | | FEM (Maxwell) | BEM (Pithia) |
| 140 T/m | 17.3 kA | 11.81 T | 12.1 T |
| 150 T/m | 19.25 kA | 13.26 T | 13.5 T |

*Table 1*. Magnetic flux density

### Structural Analysis

A structural analysis was implimented in order to determine the structural integrity of the magnet. Six loadsteps (LS) were considered in the FEM (*Figure 6*).


*Figure 6*. Loadsteps

The Azimuthal Coil Stress (MPa) evolution for the six load steps is shown in *Figure 7*. The stress gradients are smooth and very symmetric and the peak stress remains below 160 MPa at all times. The Radial deformation (mm) on the vertical pole turns (VP), mid-turns (MT) and horizontal pole turns (HP) of the inner (IL) and outer layer (OL) of the coil is shown in *Figure 8*. The local sensitivity chart of *Figure 9* shows graphically the impact of each input parameter change on the coil peak stress.

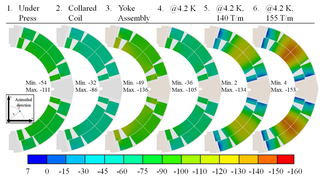


*Figure 7*. Azimuthal coil stress evolution

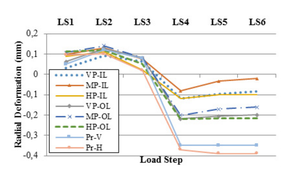


*Figure 8*. Radial deformation

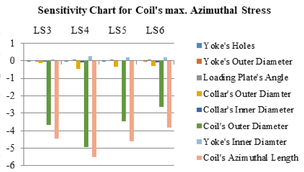


*Figure 9*. Local sensitivity chart

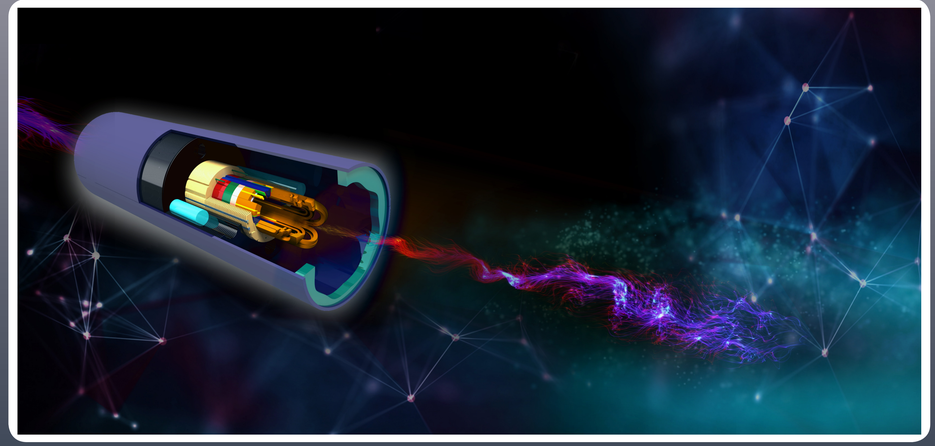

## 3D Model

The scope of the 3D model is to focus at the end region *Figure 10* of the magnet. The length of the model was 1.55 m and several design scenarios were studied including three main parameters: (i) the end plate's thickness (ii) the introduced gap, which simulates the applied pre-load by the bullets, in the bullets-coil end plate interface and (iii) the addition of tie rods, which connect the two endplates. The design converged to a model with 4 bullets, a 50 mm thick endplate, 4 rods of ø30 and pre-tension on the bullets that corresponds to an induced gap at the bullets – coil end plate interface of 0.5 mm.

### Magnetic Analysis

Similar to the 2D electromagnetic analysis, the model is analyzed in MAXWELL (*Figure 11*), ROXIE & PITHIA. The three codes are in very good agreement (Table 2).

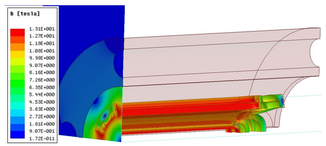


*Figure 11*. Magnetic field at 13.16 T

| Gradient | Peak Magnetic Field (T) | | | Fz (MN) per magnet | | |
|---|---|---|---|---|---|---|
| | Roxie | Pithia | Maxwell | Maxwell | Pithia | Maxwell |
| 132.6 T/m | 11.19 | 11.19 | 11.18 | 1.20 | 1.20 | 1.17 |
| 140 T/m | 11.81 | 11.81 | 11.82 | 1.31 | 1.31 | 1.30 |
| 155 T/m | 13.09 | 13.10 | 13.16 | 1.76 | 1.75 | 1.72 |

*Table 2*. Comparison of the peak magnetic field & the axial forces

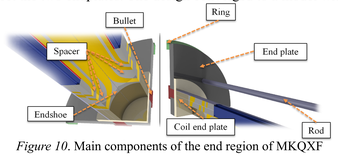


*Figure 10*. Main components of the end region of MKQXF

### Structural Analysis

Four load steps (LS3, LS4, LS5, LS6) were considered in the 3D model (*Figure 12*). Typically, the elongation of the conductor during powering shall be kept below 0.3% of its total. *Figure 13* presents the elongation of the coil's extremities. The coil deforms by 0.44 mm during powering, while the maximum allowed deformation is 0.65 mm. The 3D model replicates very well the stress field distribution in the coil of the 2D model, in any xy-plane along the straight section (*Figure 14*).

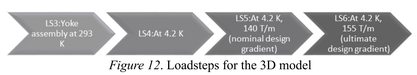


*Figure 12*. Loadsteps for the 3D model

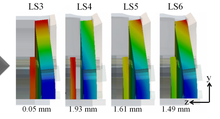


*Figure 13*. elongation of the coil's extremities [mm]

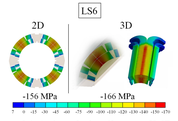


*Figure 14*. Azimuthal coil stress [MPa] and comparison with the 2D results

## Conclusions

A detailed structural optimization of the new Nb3Sn quadrupole design concept based on pole-loading and dipole-type collars has been carried out using fully parametric multi-physics FE-model and advanced CAD tools. The FEA shows that:

- Coil pre-stress can be applied in a well-controlled manner during the collaring.
- Easily tunable shimming allows the compensation of coil dimensional variations and mechanical tolerances of the magnet components.
- To counteract the very large electromagnetic forces,w the pole-loading concept provides the "tuning knobs" to tailor the coil pre-stress such that it is the highest at the pole and the lowest at the coil mid-plane at 0-current.
- The tapered-shape of the mid-plane poles together with the dipole-type collars makes it possible to carry out the collaring process in a dipole-type press and simultaneously over the entire coil length. The very rigid collars minimize the elliptic deformation after the collaring.
- The horizontally split iron yoke with a closed gap at operating temperature up to the ultimate design gradient of 155 T/m provides a very rigid structure around the coils minimizing any conductor movements and distortions from the ideal coil geometry.
- The Al-bars control the yoke gap during the assembly phase and limit the stress level in the coils.
- The stainless steel shell assembly parameters are achievable and the stresses remain at an acceptable level at all times.

The sensitivity analysis shows that the tolerances used in the study, originating from the 11 T dipole experience, create a design space, which is within the acceptable limits for all components.

- The dimensional tolerances on the coil size play the most important role on the maximum coil stress level, underlining the need for high precision metrology of the coils to carefully determine the assembly parameters.
- During the model magnet phase the shims can easily be adjusted to generate the required pre-stress levels and to compensate for the field errors. These data can then be used at a later stage to adjust the coil fabrication tooling to meet both mechanical and magnetic requirements.
- The mechanical design of the end region, including four tie rods, four bullets per side and a 50mm thick end plate, provides the necessary rigidity to the structure and minimizes effectively the elongation of the coil.
- The 3D model confirms the 2D results and the overall behavior of the structure.

## REFERENCES


[1] M. Karppinen, "New Mechanical Concept for Nb3Sn Quadrupole", CERN-ACC-2014-0244.
[2] M. Karppinen et al., "Design of 11T Twin-Aperture Nb3Sn Dipole De-monstrator Magnet for LHC Upgrades", IEEE Trans. Appl. Supercond., Vol. 22, No. 3, June 2012
[3] M. Juncho, "Support Structure Design of the Nb3Sn Quadrupole for the high Luminosity LHC", ASC-14, Charlotte, August 2014.
[4] ROXIE, https://espace.cern.ch/roxie
[5] PITHIA BEM software package, www.feacomp.com/pithia
[6] T. Gortsas, et αl., "An advanced ACA/BEM for solving 2D large-scale problems with multi-connected domains", CMES: Computer Modeling in Engineering & Sciences, 107(4), pp. 321-343, 2015
[7] C. Kokkinos et al., "The Short Model Coil (SMC) Nb3Sn Program: FE Analysis with 3D Modeling", IEEE Trans. Appl. Supercond., Vol. 22, No. 3, June 2012.
[8] C. Kokkinos, et αl., "FEA Model and Mechanical Analysis of the Nb3Sn 15 T Dipole Demonstrator," IEEE Trans. Applied Supercond., submitted for publication.